

# High-Resolution Electronic Spectra of 2-Hydroxy and 2-Aminopyridine. Perturbing Effects of the Nitrogen Atom in the Aromatic Ring

David R. Borst, Joseph R. Roscioli, and David W. Pratt\*

Department of Chemistry, University of Pittsburgh, Pittsburgh, Pennsylvania 15260

Received: November 8, 2001; In Final Form: February 14, 2002

High resolution, rotationally resolved electronic spectra of 2-hydroxypyridine (2HP) and 2-aminopyridine (2AP; at  $\sim 277$  and  $\sim 299$  nm, respectively) have been observed and fit using rigid-rotor Hamiltonians to within lifetime-limited resolutions of 170 and 120 MHz, respectively. The derived values of the rotational constants are very similar to those of phenol and aniline. However, 2HP and 2AP each exhibit inertial axis tilting, large rotations of their  $S_1-S_0$  electronic transition moments, and intramolecular hydrogen bonds, making them very different from their hydrocarbon analogues. Possible reasons for this behavior are discussed.

## Introduction

Understanding the active structures within biological molecules is integral to understanding the function and interactions of such molecules within living organisms. Ring structures containing nitrogen atoms are quite common in biological systems and provide an excellent forum for discussion of lone-pair electron effects. Such effects may play an important role in noncovalent interactions of heteroatomic rings with one another, and with other hydrocarbon aromatic rings in larger macromolecules.<sup>1</sup>

Examples of such structures include 2-hydroxypyridine (2HP) and 2-aminopyridine (2AP). Both contain in-ring nitrogen atoms, along with either *ortho* hydroxy or amino groups. 2HP, the enol tautomer of 2-pyridone (2PY), contains three potential hydrogen bonding (HB) sites: the in-ring nitrogen, the  $-OH$  group, and the  $\pi$  cloud of the aromatic ring. The corresponding active sites within 2AP are identical to those within adenine.

Both molecules have been extensively studied using a variety of high-resolution gas-phase techniques. Microwave spectra of both 2HP and 2PY have been observed and assigned.<sup>2</sup> Only the Z isomer of 2HP was detected; the absence of the E isomer suggests that an intramolecular HB preferentially stabilizes the former.<sup>3,4</sup> Kydd and Mills<sup>5</sup> measured the microwave spectrum of 2AP and found that, although the  $-NH_2$  group is out-of-plane ( $31.6^\circ$ ), one hydrogen is  $0.7 \text{ \AA}$  closer to the plane containing the ring. Electronic spectra of 2HP and 2PY also have been observed and assigned,<sup>6</sup> the latter at high resolution.<sup>7</sup> In 1970, Hollas, et al.<sup>8</sup> described the rotational band contours in the electronic spectra of three isotopomers of 2AP. Additionally, later SVL fluorescence studies of 2AP and some of its deuterated isotopomers<sup>9</sup> provided strong evidence for the existence of appreciable hydrogen bonding between the ring nitrogen and a hydrogen atom of the  $NH_2$  group.

Described herein are the fully resolved electronic spectra of 2HP and 2AP, from which is derived new structural information about their  $S_0$  and  $S_1$  electronic states, from the determined values of their moments of inertia. New information also is obtained about the electronic distributions in the two states, from the observed  $S_1-S_0$  transition moment orientations. The results

show that 2HP and 2AP are quite different from their hydrocarbon analogues, phenol and aniline, and suggest that these differences may be relevant to their biological behavior.

## Experimental Section

2HP and 2AP were purchased from Aldrich and used as received. Experiments at low resolution were performed as described previously.<sup>10</sup> Briefly, the sample was heated to  $150^\circ\text{C}$ , entrained in 60 psi of helium, and expanded into a vacuum chamber ( $10^{-5}$  Torr) through a 1 mm diameter pulsed valve (General Valve Series 9) operating at 10 Hz. The expansion was crossed by the frequency doubled output of a dye laser (Quanta Ray PDL-1), pumped by the second harmonic of a  $Nd^{3+}$ :YAG laser (Quanta Ray DCR-1A), also operating at 10 Hz. Fluorescein 548 laser dye was used to perform the 2HP experiment, and kiton red was used to perform the 2AP experiment. The resulting fluorescence was collected by a PMT, processed by a boxcar integrator, and digitally recorded by a data acquisition computer.

High-resolution spectra were obtained using a CW molecular beam spectrometer described in detail elsewhere.<sup>11</sup> The present conditions were as follows. A  $\sim 1$  g sample of 2HP or 2AP was heated to  $185^\circ\text{C}$  and entrained in  $\sim 850$  Torr He. The mixture was expanded through a  $280 \mu\text{m}$  quartz nozzle held at  $15-20^\circ\text{C}$  into a vacuum chamber, skimmed about 2 cm downstream of the nozzle before entering a second differentially pumped chamber, and probed 10 cm downstream of the nozzle with a CW laser. The excitation source was an  $Ar^+$  pumped CW single frequency (fwhm  $\sim 1$  MHz) tunable ring dye laser operating with rhodamine 110 dye (for 2HP) or rhodamine 6G dye (for 2AP) and frequency-doubled by an intracavity BBO (2HP) or  $LiIO_3$  (2AP) crystal. Typical powers used were  $300 \mu\text{W}$  in the UV. The spectra were recorded at an acquisition rate of 50 Hz over a 2000 second scan. Four signals were collected. The PMT signal was collected with spatially selective optics using photon counting and stored on a data acquisition computer. A signal from a near-confocal interferometer having a mode-matched free spectral range of  $599.5040 \pm 0.005$  MHz in the UV was collected to perform relative frequency calibration. The absorption spectrum of  $I_2$  was collected to determine the absolute transition frequencies, which are accurate to  $\pm 30$  MHz. Finally,

\* To whom correspondence should be addressed. E-mail: pratt@pitt.edu. Fax: 412/624-8611.

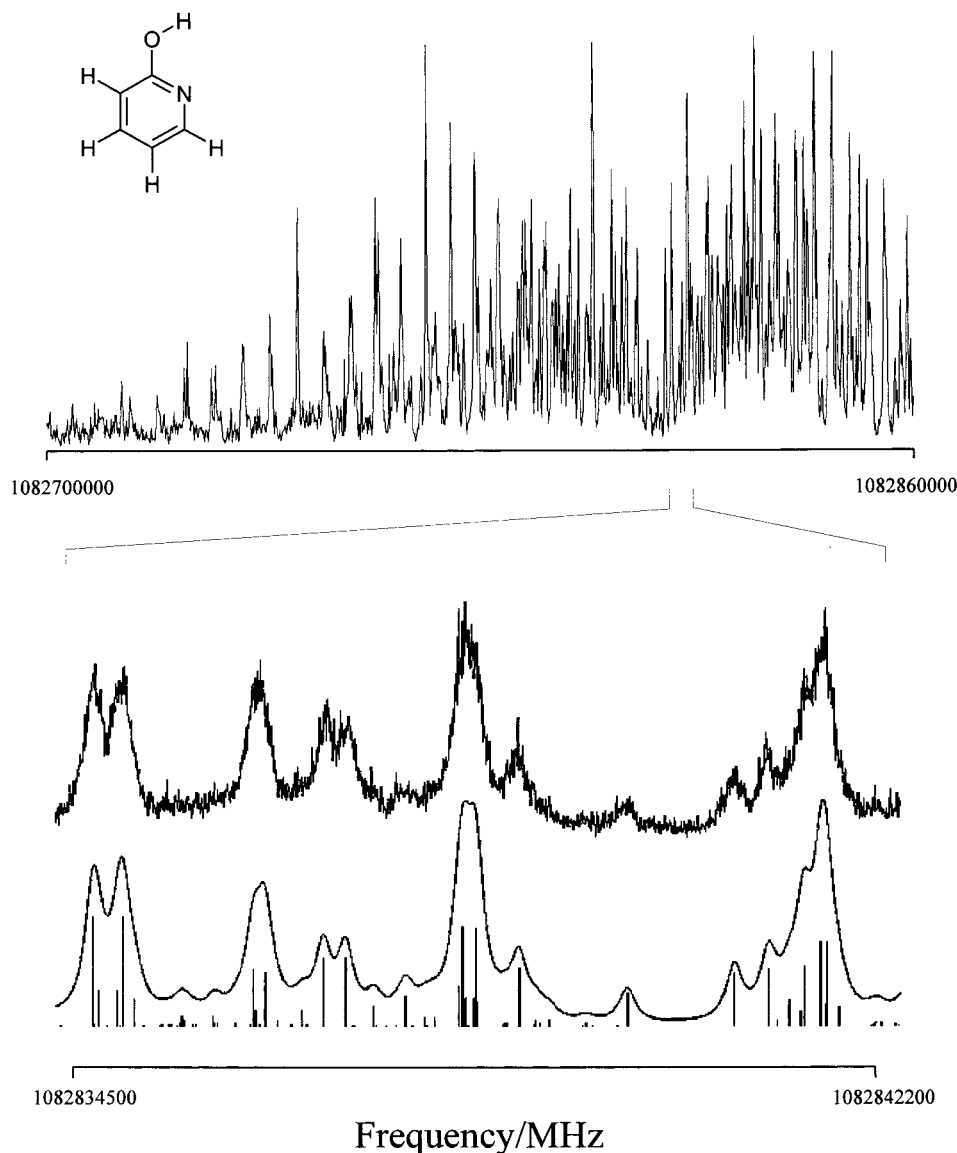


**Figure 1.** Rovibronic  $S_1-S_0$  spectrum of 2-hydroxypyridine at  $\sim 277$  nm. The inset shows a portion of the experimental spectrum at full resolution, together with two simulations, with and without superimposed line shape functions. A total of 173 lines were included in the fit, resulting in an OMC of 5.5 MHz. The single rovibronic line width is  $170 \pm 10$  MHz.  $T = 4.8$  K.

the power signal was collected to normalize the PMT signal. Under these conditions, typical single rovibronic line widths are  $\sim 30$  MHz, principally limited by the Doppler effect.

Supplementing the experimental work, we also performed *ab initio* calculations using density functional theory. Geometry optimizations of the ground state were accomplished using B3LYP/6-31G\*, and  $S_1-S_0$  transition moment orientations were determined using CIS/6-31G\* methods. All calculations were performed using the Gaussian 98<sup>12</sup> suite of electronic structure programs on Indigo workstations or using G98W on personal computers.

## Results

Figure 1 shows the first  $5\text{ cm}^{-1}$  in the high-resolution spectrum of the  $0_0^0$  band in the  $S_1-S_0$  electronic transition of 2HP, at  $36\,117\text{ cm}^{-1}$  ( $\sim 277\text{ nm}$ ).<sup>6</sup> (The entire spectrum spans about  $\sim 7\text{ cm}^{-1}$  under our experimental conditions.) Immediately apparent is the fact that this band is an *ab*-hybrid band because the spectrum contains both parallel and perpendicular transitions. Thus, to fit the spectrum, we independently simulated *a*-type and *b*-type bands and varied their relative intensities until they

matched those that were experimentally observed. Both simulations utilized the same sets of rotational constants for the  $S_0$  and  $S_1$  electronic states. We used the microwave values of these constants<sup>2</sup> for the ground states; these were not varied in the fit. We used estimates of these constants for the excited state, on the basis of the known values for the closely related molecule phenol.<sup>13</sup> These were varied in a least-squares fashion in the fit, until the difference between the observed and calculated line positions was minimized.

An additional challenge emerged as the fit of the  $0_0^0$  band of 2HP was nearing completion. Despite our best efforts, certain experimental line intensities were not well reproduced in several simulations of the hybrid band spectrum, using a large variety of possible TM orientations and rotational temperatures. This challenge was met by assuming that the inertial axes of 2HP in the two electronic states are not coincident. This effect, termed "axis tilting",<sup>14</sup> was also encountered in an analysis of the corresponding spectrum of the 2HP tautomer, 2PY.<sup>7</sup> As discussed there, axis tilting leads to anomalous line intensities in a fully resolved spectrum and may be accounted for by adding additional, off-diagonal terms in the excited-state Hamiltonian.

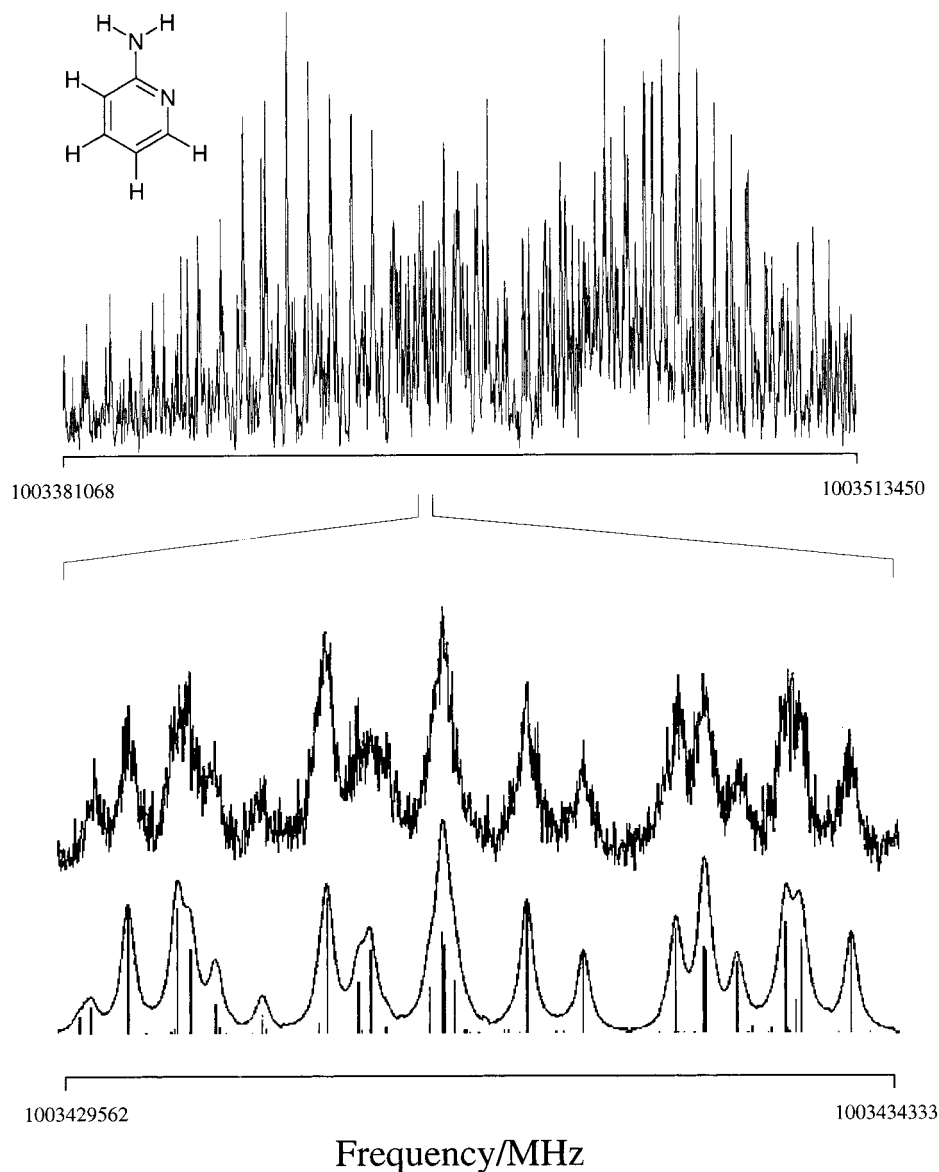


**Figure 2.** Rovibronic  $S_1$ – $S_0$  spectrum of 2-aminopyridine at  $\sim 299$  nm. The inset shows a portion of the experimental spectrum at full resolution, together with two simulations, with and without superimposed line shape functions. A total of 74 lines were included in the fit, resulting in an OMC of 6.5 MHz. The single rovibronic line width is  $120 \pm 10$  MHz.  $T = 5.0$  K.

Following this procedure in the present case leads to the conclusions that the  $S_1$ – $S_0$  TM in 2HP makes an angle of  $\theta = \pm 53 \pm 3^\circ$  with respect to  $a$  and that the inertial axes tilt in the opposite direction by  $\phi = \mp 1.3 \pm 0.10$  when the photon is absorbed.

The quality of our fit is revealed by comparisons of portions of the experimental and computed spectra. An example is also shown in Figure 1. Illustrated there is an  $\sim 8$  GHz portion of the R branch at full experimental resolution and two simulations, with and without convoluted line shape functions. Although congested, individual transitions could be identified in the spectra, and analyses of these with Voigt line shape functions yielded Gaussian and Lorentzian line widths of  $\sim 30$  and  $\sim 170$  MHz, respectively. The Lorentzian width corresponds to a lifetime of  $\sim 1$  ns.

A similar procedure was followed for 2AP. Its  $S_1$ – $S_0$  origin band is at  $33\,471\text{ cm}^{-1}$  ( $\sim 299$  nm),<sup>8</sup> red shifted by  $2646\text{ cm}^{-1}$  from the corresponding band in 2HP. Figure 2 shows the high-resolution spectrum of this band in 2AP. It is also an  $ab$ -hybrid band and exhibits a small axis tilt, as well. Fits of this spectrum yielded a TM orientation of  $\theta = \pm 58 \pm 3^\circ$  and a tilt angle of

$\phi = \mp 1.4 \pm 0.2^\circ$ . The value of  $\theta$  in 2AP is significantly different from that in 2HP ( $53^\circ$ ). Individual rovibronic lines also could be identified (cf. Figure 2) and fit to line shape functions, yielding Gaussian and Lorentzian widths of  $\sim 30$  and  $\sim 120$  MHz, respectively. The Lorentzian width corresponds to a lifetime of  $\sim 1.5$  ns, slightly longer than that in 2HP.

Table 1 lists the inertial parameters derived from the fits of the origin bands in the high-resolution  $S_1$ – $S_0$  electronic spectra of 2HP and 2AP. As noted, the values shown for the  $S_0$  state are from microwave studies; those for the  $S_1$  state were derived from least-squares fits of the spectra in Figures 1 and 2. Comparing the rotational constants for the two states, of the two molecules, we see that they are remarkably similar, as expected. 2AP has slightly smaller values of  $A$ ,  $B$ , and  $C$ , as a consequence of its slightly larger moments of inertia about the three principal axes, in both states. Furthermore the values of  $\Delta A$ ,  $\Delta B$ , and  $\Delta C$  for the two molecules also are very similar.  $\Delta A$  is large and negative, whereas  $\Delta B$  and  $\Delta C$  are both relatively small, with different signs. These trends reflect, of course, the fact that the photon-induced changes in the geometries of 2HP and 2AP are qualitatively the same.

**TABLE 1: Inertial Parameters of 2-Hydroxypyridine (2HP) and 2-Aminopyridine (2AP) in Their Ground ( $S_0$ ) and Electronically Excited ( $S_1$ ) States**

parameter	$S_0^a$	$S_1$	$S_1-S_0$
2HP			$\nu_0 = 36118.69(2) \text{ cm}^{-1}$
A, MHz	5824.95	5467.1(1)	-357.9
B, MHz	2767.53	2780.5(1)	13.0
C, MHz	1876.16	1844.6(1)	-31.6
$\Delta I, \mu\text{Å}^2$	-0.003	-0.212(23)	band type $a:b=36:64$
$\kappa$	-0.548	-0.483	$\theta(a) = \pm 53 \pm 3^\circ$
2AP			$\nu_0 = 33471.39(2) \text{ cm}^{-1}$
A, MHz	5780.34	5439.9(1)	-340.5
B, MHz	2733.57	2771.7(1)	38.2
C, MHz	1857.66	1837.7(1)	-20.0
$\Delta I, \mu\text{Å}^2$	-0.258	-0.231(23)	band type $a:b=28:72$
$\kappa$	-0.553	-0.481	$\theta(a) = \pm 58 \pm 3^\circ$

<sup>a</sup> Microwave values. See refs 2 and 5.

**TABLE 2: Inertial Parameters of Phenol and Aniline in Their Ground ( $S_0$ ) and Electronically Excited ( $S_1$ ) States**

parameter	$S_0^a$	$S_1^{b,c}$	$S_1-S_0$
phenol			$\nu_0 = 36348.7 \text{ cm}^{-1}$
A, MHz	5650.515	5313.6	-336.9
B, MHz	2619.236	2620.5	1.3
C, MHz	1789.855	1756.1	-33.8
$\Delta I, \mu\text{Å}^2$	-0.0309	-0.18	band type $b$
$\kappa$	-0.540	-0.514	$\theta(a) = \pm 90^\circ$
aniline			$\nu_0 = 34029.19 \text{ cm}^{-1}$
A, MHz	5617.40	5286.9	-330.5
B, MHz	2593.83	2633.8	39.9
C, MHz	1777.04	1759.4	-17.6
$\Delta I, \mu\text{Å}^2$	-0.406	-0.232	band type $b$
$\kappa$	-0.575	-0.504	$\theta(a) = \pm 90^\circ$

<sup>a</sup> Microwave values. See refs 16 and 17. <sup>b</sup> UV values for phenol. See ref 13. <sup>c</sup> UV values for aniline. See ref 18.

Comparing these results to those obtained previously, we note that our  $\Delta A$ ,  $\Delta B$ , and  $\Delta C$  values for 2AP agree very well with the earlier contour studies of Hollas et al.<sup>9</sup> We also note that significant discussion has been given, elsewhere, of the increasing tendency for  $\Delta B$  to be positive in substituted benzenes, as one goes from increasingly double C-F to C-O to C-N bonds in the  $S_1$  state.<sup>15</sup> 2AP fits within this trend.

## Discussion

2HP and 2AP are N-heterocyclic analogues of phenol and aniline, respectively. Therefore, it is interesting to compare the properties of the four molecules in their two electronic states. Table 2 lists the band origin frequencies,  $S_1-S_0$  transition moment orientations, and rotational constants of phenol and aniline<sup>13,14</sup> for comparison with those of 2HP and 2AP, listed in Table 1. The  $S_1-S_0$  band origins of the N-heterocyclics are each red shifted with respect to their hydrocarbon analogues, by relatively small amounts (230 and 558  $\text{cm}^{-1}$ , respectively). Their rotational constants are also qualitatively the same, with the N-heterocyclics having slightly larger A, B, and C values (smaller moments of inertia). The changes in these constants that occur when the molecules absorb light ( $\Delta A$ ,  $\Delta B$ , and  $\Delta C$ ) also are very similar. However, the  $S_1-S_0$  transition moment orientations of 2HP and 2AP are very different from their hydrocarbon analogues. Phenol and aniline each exhibit  $S_1-S_0$  transitions that are pure  $b$ -type, with  $\theta(a) = \pm 90^\circ$ , whereas 2HP and 2AP each exhibit  $S_1-S_0$  transitions that are  $ab$ -hybrid-type, with  $\theta(a) = \pm 53^\circ$  and  $\pm 58^\circ$ , respectively. Thus, the electron distributions in 2HP and 2AP, and how they change when the photon is absorbed, must be very different from those in phenol and aniline.

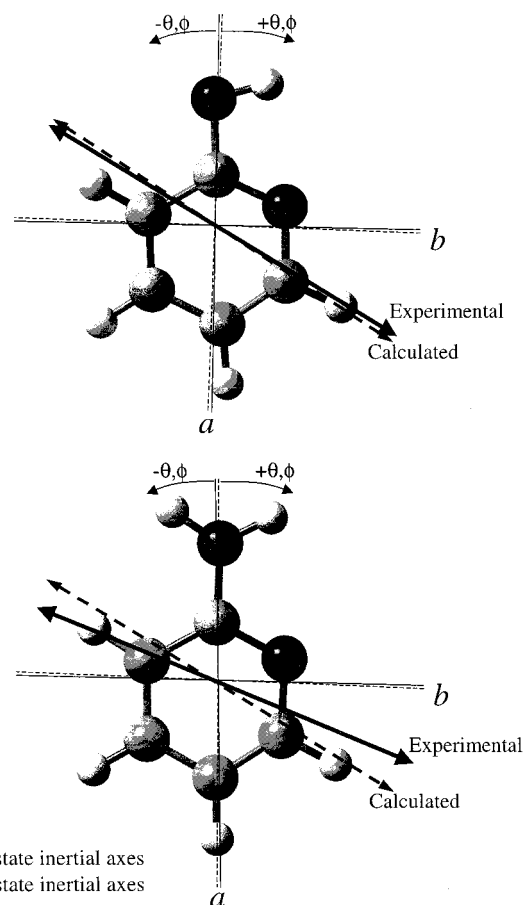


**Figure 3.** Inertial axes, transition moment, and axis tilt orientations in 2-hydroxypyridine (top) and 2-aminopyridine (bottom). The  $\theta$ -sign convention is that used for the axis tilt.

Before discussing the ways in which the  $S_1-S_0$  transitions of 2HP and 2AP are different from those of their hydrocarbon analogues, we note one important similarity: all are  $\pi\pi^*$  transitions, because they are in-plane polarized. An  $n\pi^*$  transition would be polarized perpendicular to the plane, as is the case for pyridine itself. An early band contour analysis<sup>19</sup> of the origin band of the  $S_1-S_0$  transition of pyridine- $d_1$  (at  $\sim 287 \text{ nm}$ ) showed clearly that it is a  $c$ -type band. This observation has been confirmed in the high-resolution optothermal study of pyridine in its  $S_1$  state by Becucci, et al.<sup>20</sup> Therefore, because all four transitions considered here are in-plane polarized, all are  $\pi\pi^*$  transitions.

Nonetheless, the  $S_1-S_0$  transitions of 2HP and 2AP are different, as noted before. The first issue we must address is the orientation of the TM in the molecular frame, because experiment gives only the absolute value of  $\theta$  and not its sign. (Under some conditions, the sign of  $\theta$  can be determined by experiment,<sup>21</sup> but those conditions do not exist here.) So, we turn to theory for some guidance on this issue. Ab initio calculations were performed using Gaussian 98<sup>12</sup> on both 2HP and 2AP, using the B3LYP method for the  $S_0$  state and the CIS method for the  $S_1$  state. Energy optimized geometries of each state were determined, yielding rotational constants in excellent agreement with experiment ( $\sim 0.2\%$  for the  $S_0$  state and  $\sim 2.5\%$  for the  $S_1$  state). Additionally,  $S_1-S_0$  TM orientations also were calculated, yielding the angles  $\theta = -58^\circ$  and  $-60^\circ$  for 2HP and 2AP, respectively. This shows that the TM vector is rotated in a counterclockwise fashion with respect to  $a$ , as illustrated in Figure 3. The magnitudes of the calculated angles are also in excellent agreement with experiment ( $\pm 53^\circ$  and  $\pm 58^\circ$ ,

**TABLE 3: CIS Expansion Coefficients Squared of the Principal One-Electron Excitations Contributing to the  $S_1$ - $S_0$  Transitions of 2-Hydroxypyridine (2HP), 2-Aminopyridine (2AP), Phenol, and Aniline (6-31G\* Basis Set)**

molecule	(HOMO $\rightarrow$ LUMO) <sup>2</sup>	(HOMO - 1 $\rightarrow$ LUMO + 1) <sup>2</sup>
2HP	0.8844	0.1156
2AP	0.9145	0.0855
phenol	0.7550	0.2450
aniline	0.8300	0.1700

respectively). The ab initio transition moments that agree best with the experiment cross the ring, nearly “perpendicular” to the in-ring nitrogen.

A second approach may be taken to address this issue, an approach that is also rooted in theory. Recall that 2HP and 2AP both exhibit axis tilting; the inertial axes of their  $S_0$  and  $S_1$  states are not coincident. Also recall that a principal consequence of axis tilting in a fully resolved spectrum is “anomalous” line intensities, arising from interferences between different excitation channels.<sup>7,14</sup> Which transitions gain intensity and which transitions lose intensity, is determined by the *relative* orientations of the TM vector ( $\theta$ ) and the direction of axis tilt or reorientation ( $\phi$ ). Experimentally, in the case of 2HP and 2AP, we know that  $\theta$  and  $\phi$  have opposite signs. Therefore, the sign of  $\theta$  can be determined if the sign of  $\phi$  is known.

Information about the sign of  $\phi$  is contained in the results of the ab initio calculations on the two electronic states of 2HP and 2AP. Using the atomic positions determined from the energy-optimized structures, we constructed a  $Z$  matrix for each molecule, in each state. These matrices were then diagonalized, to determine the location of the principal axes of inertia and of each of the component atoms in this coordinate system. The results for each state were then compared, to determine the direction of the axis tilt.  $S_1$ - $S_0$  excitation produces a clockwise tilt of the inertial axis in both molecules, as also shown in Figure 3. Therefore, the  $\theta$  values of 2HP and 2AP are both negative, as concluded before, because  $\phi$  is positive in both cases.

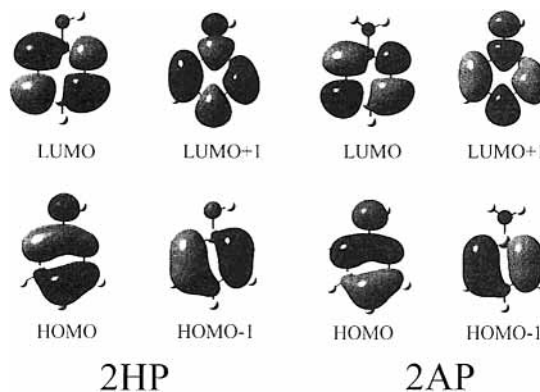
In electronic spectroscopy, the TM is the dipole moment of an oscillating charge density and, hence, is related to the wave functions of the electrons in the two states connected by the photon. Thus

$$(\mu_z)_{12} = \int \Psi_2^* \hat{\mu}_z \Psi_1 \, d\tau \quad (1)$$

Typically, the total electronic wave functions  $\Psi_1$  and  $\Psi_2^*$  may be expressed as products of the occupied and unoccupied molecular orbitals (MOs) of the system. Thus, the orientation of the electronic TM in the molecular frame is determined by the nodal patterns of the participating MOs.<sup>22</sup>

Information about the MOs that participate in the  $S_1$ - $S_0$  transitions of phenol and aniline and their *N*-heterocyclic analogues, also is contained in the results of the ab initio calculations. Table 3 lists the principal one-electron excitations that contribute to the  $S_1$ - $S_0$  transitions in all four molecules. Examining these data, we see that the dominant excitations in all four molecules are HOMO  $\rightarrow$  LUMO in type, with the next most significant contribution coming from HOMO - 1  $\rightarrow$  LUMO + 1 excitations. Thus, differences between the TM orientation in the *N*-heterocyclics and the corresponding aromatics cannot be attributed to state mixing, because all four transitions are clearly  ${}^1L_b$  in character.  ${}^1L_a$  states are derived from excitations of the HOMO - 1  $\rightarrow$  LUMO and HOMO  $\rightarrow$  LUMO + 1 type.<sup>22,23</sup>

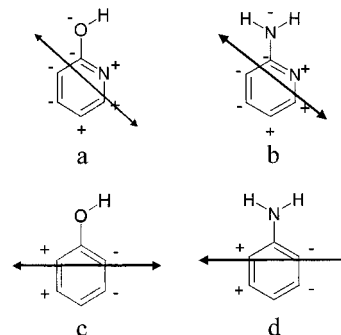
The principal factors responsible for the differences in the TM orientations are the nodal properties of the wave functions

**Figure 4.** Calculated molecular orbitals of 2-hydroxypyridine (left) and 2-aminopyridine (right).

themselves. Figure 4 shows plots of the four relevant MOs in 2HP and 2AP. The HOMO - 1 and LUMO orbitals of phenol and aniline exhibit nodes at the *para* carbon atoms,  $C_1$  and  $C_4$ . Hence, the contribution from these atoms to the product  $\Psi_1\Psi_2^*$  is negligible. In contrast, the corresponding orbitals in 2HP and 2AP do exhibit density on  $C_1$  and  $C_4$ ; the nodes in HOMO - 1 and LUMO are shifted away from these atoms. Additionally, the electron density in these orbitals on the -OH group of phenol and on the -NH<sub>2</sub> group of aniline is greatly enhanced in 2HP and 2AP, compared to the hydrocarbons themselves. There are further, minor distortions of the HOMO and LUMO + 1 orbitals in 2HP and 2AP. Thus, when one computes the transition densities  $\Psi_1\Psi_2^*$ , one finds that the nodal planes of these oscillating charge distributions are rotated significantly in 2HP and 2AP, compared to phenol and aniline. This is shown in Figure 5.

It is likely that these differences in transition densities also are responsible, in fact, for the (small) differences in the values of  $\Delta A$ ,  $\Delta B$ , and  $\Delta C$  in the four molecules (cf. Tables 1 and 2). These effects were not analyzed in detail. However, it is clear even on a cursory examination of Figure 5 that the asymmetries in the oscillating charge distributions which are shown there are also responsible for the axis tilting that is observed in the spectra of 2HP and 2AP.

What causes the asymmetries in these charge distributions? The simple answer is, obviously, the in-ring nitrogen atom, which is electronically different from the C-H bond that it replaces. In particular, the aromatic nitrogen atom has a lone pair, whereas the carbon atom does not. We believe, however, that the nitrogen atom is only “indirectly” responsible for these differences, by virtue of an attractive interaction between its lone pair and the hydrogen atom(s) of the attached group, i.e., an intramolecular hydrogen bond.

**Figure 5.** Transition densities of (a) 2-hydroxypyridine, (b) 2-aminopyridine, (c) phenol, and (d) aniline.

Positive evidence for the existence of such a bond is provided by the measured rotational constants of 2HP and 2AP and especially in the values of the inertial defects derived from them (Tables 1 and 2). 2HP and phenol both have small negative values of  $\Delta I$ , in their electronic ground states, indicating essentially planar structures. However, the  $\Delta I$  value of  $S_0$  phenol ( $-0.0309 \text{ amu } \text{\AA}^2$ ) is an order of magnitude larger than that of  $S_0$  2HP ( $-0.003 \text{ amu } \text{\AA}^2$ ). We suggest that the reason for this difference is that the OH group in phenol has much greater torsional amplitude than that in 2HP, owing to the existence of an intramolecular HB in 2HP. Further, we know from theory that *Z*-2HP is considerably more stable than *E*-2HP. A similar effect has been observed in 2-hydroxyquinoline.<sup>24</sup>

Ground-state aniline is a nonplanar molecule, owing to displacements along the out-of-plane amino inversion mode. Its inertial defect is  $\Delta I = -0.406 \text{ amu } \text{\AA}^2$ . This value also is reduced in magnitude significantly in 2AP, to  $\Delta I = -0.258 \text{ amu } \text{\AA}^2$ , again indicating an intramolecular HB. Both inertial defects decrease when the molecule is excited to the  $S_1$  state (to the nearly identical values of  $-0.232$  and  $-0.231 \text{ amu } \text{\AA}^2$ , respectively). The  $S_1$  state of aniline is known to be a quasiplanar molecule.<sup>18</sup> Thus, we conclude that the  $S_0$  state of 2AP also is planar, in the same sense, and that this is a consequence of an intramolecular HB.

The hydrogen bonding interaction is primarily electrostatic in nature. Thus, motion of electrons either toward or away from a HB site will have a significant effect on the HB itself. The nodal plane of the LUMO + 1 orbital passes through the in-ring nitrogen (Figure 4). Therefore, this atom loses electron density in the  $S_1$  state, and the intramolecular HB in this state is significantly weaker, compared to the  $S_0$  state. Consequently, torsion of the OH group in 2HP has a significantly higher amplitude, and  $\Delta I$  increases in magnitude to  $\Delta I = -0.34 \text{ amu } \text{\AA}^2$ , providing a quantitative measure of this effect.

In summary, high-resolution studies of the electronic spectra of 2-hydroxypyridine (2HP) and 2-aminopyridine (2AP) have made possible accurate measurements of the rotational constants of both molecules in their ground ( $S_0$ ) and excited ( $S_1$ ) electronic states. These constants are qualitatively similar to the two aromatic hydrocarbon analogues of 2HP and 2AP, phenol and aniline, showing that the geometries of the four molecules are largely the same. However, the electronic distributions in the two N-heterocyclics are significantly different from their hydrocarbon analogues. This is evidenced primarily by small inertial axis reorientations on  $S_1$  excitation, significantly larger rotations of their electronic transition moment vectors in the molecular plane, and intramolecular hydrogen bonds between the in-plane nitrogen and a hydrogen atom of the attached  $-\text{OH}$  or  $-\text{NH}_2$  group. Significant differences in the noncovalent interactions involving N-heterocyclic rings, compared to hydrocarbon aromatic units, are possible biological consequences of these effects, which remain to be explored.

**Acknowledgment.** This work has been supported by NSF (CHE - 9987048). We thank Michael Hollas, Tim Korter, and Jason Ribblett for helpful discussions.

## References and Notes

- (1) See, for example: McKay, S. L.; Haptonstall, B.; Gellman, S. H. *J. Am. Chem. Soc.* **2001**, *123*, 1244.
- (2) Hatherley, L. D.; Brown, R. D.; Godfrey, P. D.; Pierlot, A. P.; Caminati, W.; Damiani, D.; Melandri, S.; Favero, L. B. *J. Phys. Chem.* **1993**, *97*, 46.
- (3) E (entgegen) denotes that the substituents of highest CIP priority,<sup>4</sup> here the  $-\text{OH}$  and  $-\text{N}$  groups, at each end of the double bond are trans to one another; if the substituents are cis, the description is Z (zusammen).
- (4) Eliel, E. L.; Wilen, S. H.; Mander, L. N. *Stereochemistry of Organic Compounds*; Wiley-Interscience: New York, 1994.
- (5) Kydd, R. A.; Mills, I. M. *J. Mol. Spectrosc.* **1972**, *42*, 320.
- (6) Nimlos, M. R.; Kelley, D. F.; Bernstein, E. R. *J. Phys. Chem.* **1989**, *93*, 643.
- (7) Held, A.; Champagne, B. B.; Pratt, D. W. *J. Chem. Phys.* **1991**, *95*, 8732.
- (8) Hollas, J. M.; Kirby, G. H.; Wright, R. A. *Mol. Phys.* **1970**, *18*, 327.
- (9) Hollas, J. M.; Musa, H.; Ridley, T. *J. Mol. Spectrosc.* **1984**, *104*, 107.
- (10) Johnson, J. R.; Jordan, K. D.; Plusquellic, D. F.; Pratt, D. W. *J. Chem. Phys.* **1990**, *93*, 2258.
- (11) Majewski, W. A.; Plusquellic, D. F.; Pratt, D. W. *J. Chem. Phys.* **1989**, *90*, 1362.
- (12) Frisch, M. J.; Trucks, G. W.; Schlegel, H. B.; Scuseria, G. E.; Robb, M. A.; Cheeseman, J. R.; Zakrzewski, V. G.; Montgomery, J. A., Jr.; Stratmann, R. E.; Burant, J. C.; Dapprich, S.; Millam, J. M.; Daniels, A. D.; Kudin, K. N.; Strain, M. C.; Farkas, O.; Tomasi, J.; Barone, V.; Cossi, M.; Cammi, R.; Mennucci, B.; Pomelli, C.; Adamo, C.; Clifford, S.; Ochterski, J.; Petersson, G. A.; Ayala, P. Y.; Cui, Q.; Morokuma, K.; Malick, D. K.; Rabuck, A. D.; Raghavachari, K.; Foresman, J. B.; Cioslowski, J.; Ortiz, J. V.; Stefanov, B. B.; Liu, G.; Liashenko, A.; Piskorz, P.; Komaromi, I.; Gomperts, R.; Martin, R. L.; Fox, D. J.; Keith, T.; Al-Laham, M. A.; Peng, C. Y.; Nanayakkara, A.; Gonzalez, C.; Challacombe, M.; Gill, P. M. W.; Johnson, B. G.; Chen, W.; Wong, M. W.; Andres, J. L.; Head-Gordon, M.; Replogle, E. S.; Pople, J. A. *Gaussian 98*, revision A.9; Gaussian, Inc.: Pittsburgh, PA, 1998.
- (13) Berden, G.; Meerts, W. L.; Schmitt, M.; Kleinermanns, K. *J. Chem. Phys.* **1996**, *104*, 972.
- (14) Hougen, J. T.; Watson, J. K. G. *Can. J. Phys.* **1965**, *43*, 298.
- (15) Cvitas, T.; Hollas, J. M.; Kirby, G. H. *Mol. Phys.* **1970**, *19*, 305.
- (16) Mathier, E.; Welti, D.; Bauder, A.; Günthard, H. H. *J. Mol. Spectrosc.* **1971**, *37*, 63.
- (17) Lister, D. G.; Tyler, J. K.; Høg, J. H.; Larsen, N. W. *J. Mol. Struct.* **1976**, *23*, 253.
- (18) Sinclair, W. E.; Pratt, D. W. *J. Chem. Phys.* **1996**, *105*, 7942.
- (19) Birss, F. W.; Colson, S. D.; Ramsay, D. A. *Can. J. Phys.* **1973**, *51*, 1031.
- (20) Becucci, M.; Lakin, N. M.; Pietraperzia, G.; Salvi, P. R.; Castellucci, E.; Kerstel, E. R. *J. Chem. Phys.* **1997**, *107*, 10399.
- (21) Plusquellic, D. F.; Pratt, D. W. *J. Chem. Phys.* **1992**, *97*, 8970.
- (22) Salem, L. *The Molecular Orbital Theory of Conjugated Systems*; W. A. Benjamin, Inc.: Reading, MA, 1966.
- (23) Kroemer, R. T.; Liedl, K. R.; Dickinson, J. A.; Robertson, E. G.; Simons, J. P.; Borst, D. R.; Pratt, D. W. *J. Am. Chem. Soc.* **1998**, *120*, 12573.
- (24) Held, A.; Plusquellic, D. F.; Tomer, J. L.; Pratt, D. W. *J. Phys. Chem.* **1991**, *95*, 2877.